Mechanism of salt tolerance in endangered semi-mangrove plant Barringtonia racemosa: anatomical structure, photosynthetic and fluorescence characteristics

Ju Hu
Yulin Normal University
Xu Deng
Yulin Normal University
Caihong Bai
Yulin Normal University
Lin Li
Yulin Normal University
Xiuling Yang
Yulin Normal University
Chunxiao Lan
Yulin Normal University
Haiyan Zhong
Yulin Normal University
Xiaohui Tan
Guangxi Academy of Agricultural Science
Fang Liang
liangfang360@ylu.edu.cn

Yulin Normal University

Article

Keywords:

Posted Date: February 10th, 2023

DOI: https://doi.org/10.21203/rs.3.rs-2531933/v1

Additional Declarations: No competing interests reported.

Version of Record: A version of this preprint was published at 3 Biotech on March 8th, 2024. See the published version at https://doi.org/10.1007/s13205-024-03943-6.

Abstract

Barringtonia racemosa is a rare and endangered semi-mangrove plant with salt tolerance (≤ 25‰ salt). However, mechanisms governing the salt tolerance has not been elucidated. Therefore, biomass, photosynthetic and fluorescent characteristics, and anatomical structure of _B. racemosa_ were studied to investigate the mechanism of salt tolerance. The results showed that stem dry weight decreased under high salt stress (30‰-40‰). Net photosynthetic rate, intercellular CO_2 concentration of _B. racemosa_ significantly decreased under 35‰ and 40‰ salt treatments, Fv/Fm decreased significantly under 40‰ salt stress, ΦPSI decreased significantly under 35‰ and 40‰ salt stress. The thickness of epidermis of root significantly increased under 25‰ and 40‰ salt treatments. The outer cortex and stele diameters of root significantly increased, under high salt treatments. The xylem and phloem of stem significantly increased under salt treatments, while the cambium and cortex of stem significantly decreased under salt treatments. The width of the increment or stable palisade tissue and spongy mesophyll. Therefore, stable net photosynthetic rate and intercellular CO_2 concentration, increment of Fv/Fm and ΦPSI, the increment or stable palisade tissue and spongy mesophyll of leaf and the increment of epidermis, outer cortex, and stele diameter of root could contribute to salt tolerance of _B. racemosa_.

Introduction

Salt stress, the most prevalent abiotic stress, affects physiological, biochemical, and molecular processes in plants and reduces their productivity[1,2], it can cause ion imbalance, osmotic stress, oxidative stress, water and nutrient deficiency in plants, and damage biological macromolecules, growth retardation, and even lead to death[3–6]. Salt tolerant plants play an important role in saline soil remediation and utilization, they can improve the soil structure and fertility with the characteristics of energy saving, stable and lasting effects, and almost no pollution to the environment[7,8].

In salt tolerant plants, three main mechanisms of salt tolerance have been proposed: tolerance to osmotic stress, sodium (Na) exclusion from leaf blades, and tissue tolerance[7]. Salt tolerant plants can improve their photosynthetic capacity by modifying and redistributing electron transport between photosystems, and change root, stem, and leaf subcellular structural to improve the stability of the photosystem to improve salt stress tolerance in field conditions[8].

Sea level is rising from year to year, and the coastal saline soil area increasing in China, the salt concentration reached about 30‰-40‰ in the South China Sea[9], however, the plant species which are suitable for coastal mudflats are limited[10–12]. Semi-mangrove plants grow in the intertidal zone of tropical and subtropical coastlines and provide a natural barrier to the coast in China[13,14]. *Barringtonia racemosa*, an evergreen tree belonging to the Lecythidaceae genus *Barringtonia*, is an endangered semi mangrove ornamental plant[15], and it is a typical tropical and subtropical coastal plant, widely distributed in Guangxi, Guangzhou, Hainan, Taiwan provinces in China[16]. Previous studies found that *B. racemosa* was tolerant to salt stress (≤ 25‰)[17–20], the growth of plant was not impacted by salt stress (≤ 25‰),

however, the mechanism is not clear. The objective of this study is to investigate the mechanism of salt tolerance of *B. racemosa* by studying the photosynthetic and fluorescence characteristics, and anatomical structure under salt stress.

Materials And Methods

Plant materials. The seeds of *B. racemosa* used in the following experiments were collected from the natural forest in Qili village, Zhonghe town, Danzhou city, Hainan province, China (N19°76', E109°38'). The formal identification of *B. racemosa* was undertaken by Taiping He who is a professor in plant taxonomy in Guangxi University, the plant materials were compared with the specimens (AU058561) of *B. racemosa* in plant herbarium of School of Life Science, Xiamen University. Voucher specimens (YLSY-BR001) of *B. racemosa* were deposited in the Southeast Guangxi Distinctive Medicinal Plant Herbarium, Yulin Normal University. The seeds were sown in nursery shed in greenhouse in Yulin Normal University, Guangxi province, China (N22°64', E110°14'). Upon reaching a height of about 20 cm, the seedlings were transplanted into pots (one plant in each pot) with orchard soil and coconut bran (1:1, volume ratio) for growth. Finally, uniform 2-year-old seedlings (80 cm height) were selected for further study.

Experimental design. There were seven sea salt treatments which included control (0‰), 15‰, 20‰, 25‰, 30‰, 35‰, 40‰ sea salt, respectively. The solutions with different sea salt concentrations were prepared by dissolving sea salt to tap water. Then the solution was put in the tank of automatic tide device which was used to mimick tide, this device had a plant cultivation tank, a timer, a water pump, a filtering system, a fill light system and a shading system. The pumping time was controlled by the timer automatically. The seedlings in the pots were submerged (just above the pot) for 6 h from 9:00am to 15:00pm every day, plants were treated 9 days (from 5 May 2020 to 13 May 2020) in total. After 9 days of salt treatments, three plants were selected from each treatment for all measurements.

Determination of photosynthetic and fluorescence characteristics. After 9 days of salt treatments, during the period of 9:00–11:00 am, three leaves were randomly selected from each seedling to obtain the net photosynthetic rate (Pn), intercellular CO_2 concentration (Ci), stomatal conductance (Gs) and transpiration rate (Tr) with a portable photosynthetic analyzer (TPS-2, PP Systems, New York, USA); quantum yield (Fv/Fm), non-photochemical quenching (NPQ), PSII actual photo-chemical quantum yield (ΦPSII) and PSI actual photochemical quantum yield (ΦPSI) under steady-state conditions were measured by CF Imager chlorophyll fluorescence imaging system (Technologica, Ltd., UK)[21], each leaf was measured three times.

Anatomical analysis. Root, stem and leaf of each seedling were fixed in FAA (formalin: 70% ethanol: glacial acetic acid = 1: 18: 1) solution, and embedded in paraffin, the embedded roots, stems and leaves were sectioned at 3 μm, the sections were sequentially placed in xylene for 20 min twice, absolute ethanol for 5 min twice, and 75% alcohol for 5 min. Then, the slices were stained with 5 g L^{-1} safranin solution for 1 to 2 h and Fast Green for 30 to 60 s. The slices were mounted with neutral gum and dried at 40°C for 12 h. Roots, stems and leaves sections examined under a light microscope (Olympus, BH2 REC, Tokyo,

Japan), and cellSens Standard software was used for photograph and analysis. Image-Pro Plus 6.0 (Media Cybemetics U.S.A.) was used for anatomical structure analysis.

Determination of biomass and root-shoot ratio. Root, stem and leaf of each seedling was separated, fresh weight was measured, then they were dried at 105°C for 30 min, and dried at 70°C to a constant weight (approximately 48 h). Dry weights of the root (RDW), stem (SDW) and leaf (LDW) were measured. Total dry weight (TDW) and root/shoot (R/S) ratios calculated using the following formulae[22]: TDW = RDW + SDW + LDW; R/S = RDW/(SDW + LDW).

Statistics and analysis. All statistical analyses were performed with SPSS Statistics 22 (SPSS Inc., Chicago, USA), the data were analyzed by one-way analysis of variance (ANOVA) and least significant difference test (Duncan, $P < 0.05$). OriginPro 2021b 9.8.5.201 (OriginLab, Inc., Massachusetts, USA) was used to draw the figures.

Results

Biomass and root-shoot ratio.

Compared with control, 30‰-40‰ salt stress significantly reduced SDW and TDW (Table 1), while 15‰ salt stress significantly increased TDW. No significant differences were found in RDW and LDW and RSR across all salt treatments and control.

Photosynthetic and fluorescence characteristics.

Photosynthetic parameters of Barringtonia Racemosa, Pn, Tr, Gs and Ci, under different salt treatments, were showed in Table 2. Under 35‰ and 40‰ salt treatments, Pn significantly decreased by 63.38% and 65.10%, respectively, and Ci decreased by 17.42% and 18.22%, respectively, compared with control. There were no significant differences in Tr and Gs of B. racemosa between under all salt treatments and control.

Significant lower Fv/Fm were observed only after treatment with 40‰ salt, compared with the control (Table 3), the seedlings treated with 35‰ and 40‰ salt had significantly lower ΦPSI than the control, and ΦPSI reached the lowest value under 40‰ salt treatment. 20‰, 30‰, 35‰ and 40‰ salt treatments significantly decreased NPQ. No significant differences were observed in ΦPSII across all salt treatments and control.

Anatomical analysis of root, stem and leaf of B. racemosa.

The root shrinked under salt stress, especially under 35‰ and 40‰ (Figure 1). The thickness of epidermis (Ep) significantly increased under 25‰ and 40‰ salt treatments compared with control (Table 4). Compared with control, except for 30‰ salt treatment, the outer cortex (Ex) significantly decreased under salt treatments. Compared with control, the St diameters under 15‰ and 25‰ salt treatments significantly increased, while the stele (St) diameters under 30‰, 35‰ and 40‰ salt treatments significantly decreased.

For stem, under salt stress, xylem (Xy) and phloem (Ph) under salt treatments were significantly thicker than that under control, except for Xy under 20‰ and Ph under 40‰ salt treatment (Fig. 2, Table 5), the highest value of Xy (3368.06 μm) and Ph (782.95 μm) were observed in 30‰ and 25‰ salt treatments, respectively. Cambium (Ca), and Cortex (Co) under salt treatments was significantly thinner than that under control (Table 6, Fig. 3). The lowest value of Ca (48.22 μm) and Ph (268.81 μm) were observed in 20‰ and 30‰ salt treatments, respectively.

B. racemosa stem under salt stress.

In terms of leaf, significant thinner upper epidermis (Ue) were observed after treatment with 15‰, 20‰, 25‰ and 35‰ salt compared with the control, and significant thinner lower epidermis (Le) were observed after treatment with 20‰ and 25‰ salt compared with the control (Figure 3, Table 6). Significant thicker midrib bund (Mb) were observed after treatment with 15‰, 20‰, 25 ‰ and 35‰ salt compared with the control. For palisade tissue (Pt) and spongy mesophyll (Sm), compared with control, 15‰ and 35‰ salt significantly increased the thickness of Pt, while 25‰ and 40‰ salt significantly decreased the thickness of PT; 15‰ and 30‰ significantly increased the thickness of SM, while 35‰ salt significantly decreased the thickness of Sm. No significant differences were observed in the width of Pc across all salt treatments and control.

Correlation between photosynthetic, fluorescence parameters and biomass, root-shoot ratio.

As shown in Fig. 4, SDW had significant positive correlation with Tr, Ci and ΦPSI, SDW had a significant positive correlation with ΦPS . RSR had significant negative correlation with Tr, Ci, ΦPS and ΦPSI. No significant correlations were observed between photosynthetic, fluorescence parameters and root day weight, total dry weight.

Discussion

Biomass (dry weight) was a comprehensive response to stress in plants[23]. Under salt stress, the different parts of plants could change the biomass to adapt to the environment and maintain their growth[24,25]. In this study, the stem dry weight decreased under 30‰-40‰ salt treatment, which was the main reason that resulted in significant lower total dry weight compared with control. This is consistent with the results in *Suaeda salsa*[26], *Avena sativa*[27] and *Gossypium hirsutum*[28] in response to salt stress. However, no significant differences were found in root and leaf dry weight and root-shoot ratio under all salt treatment and control. The results indicated that *B. racemosa* could significant reduce stem dry weight in response to high concentration salt stress (30‰-40‰).

Generally, salt stress will inhibit plant photosynthesis, Liu et al.[29], Zhao et al.[30] and Zhou et al.[31] found that Pn, Gs, Tr and Ci of mangrove plants *Elaeagnus angustifolia*, *Magnolia wufengensis* and *Gymnocarpos przewalskii* decreased under salt stress. In this study, Pn and Ci of *B. racemosa* did not change significantly under treatment with 30‰ or less salt, while they significantly decreased under 35‰ and 40‰ salt treatments, Tr and Gs did not change significantly across all salt treatments and

control. Therefore, Pn of *B. racemosa* declined mainly due to reduction of Ci, and the correlation between stem dry weight and Ci was significant, which was one of the reasons that stem dry matter reduced under high salt stress.

Chlorophyll fluorescence was very sensitive to salt stress and played an important role in the absorption, transmission, distribution, dissipation and conversion of light energy in the light system[32]. Chlorophyll fluorescence is a nonintrusive indicator for rapid assessment of adaptability and tolerance of plants under abiotic stress[33]. Fv/Fm is an important indicator of the efficiency and utilization of excitation energy captured by PSII[34]. In this study, the Fv/Fm of *B. racemosa* did not decrease significantly until the salt concentration reached 40‰, which indicated that high concentration salt stress forced the leaf to have a photoinhibition, and the light energy used for photochemical reaction decreased. Zhou et al.[31] also found that Fv/Fm of *G. przewalskii* significantly decreased under high salt stress. Plants could effectively regulate light energy and maintain their normal life activities under normal growth conditions, while the stomata of plant leaves were closed and photosynthesis was blocked, causing an imbalance between PSI and PSII and the demand for photoelectrons under stress[3]. In this study, ΦPSI significantly decreased when the salt concentration reach 35‰ and 40‰, which indicated that the photosynthetic apparatus of ΦPSI were seriously damaged with high salt concentration stress. In addition, ΦPSI significantly correlated with stem dry weight, this also contributed to stem dry weight reduction.

The anatomical analysis in this study observed that the thickness of palisade tissue and spongy mesophyll significantly increased or did not change significantly under salt treatments (especially ≤ 30‰), which could lead to these photosynthesis and fluorescence variation under salt stress. Because that thick palisade tissue could improve the photosynthetic efficiency of leaves[35], large veins and parenchyma cells could help leaves to improve water transport efficiency and water storage capacity, respectively[36,37]. Furthermore, in previous study, the anatomical structure of roots and stems of plants are related to the salt tolerance[38]. The changes of anatomical structure helped plants to improve the water storage, transportation and photosynthetic capacity of plants, alleviate salt damage, and maintain growth, development and physiological functions[36]. The increment of epidermis and cortex of *Tamarix ramosissima* roots under salt stress determines could block more Na^+ out of roots[39]. The well-developed cortex and epidermis of young roots of wheat was an important feature to adapt to salt stress, which could inhibit harmful ions from entering root cells and effectively alleviate salt damage[40]. In this study, the width of Ep and St diameter significantly increased under around 25‰, which could contributed the salt tolerance of *B. racemosa.* However, under higher salt stress (especially 40‰), Ep, Ex and St diameter decreased, which could impact the water and nutrients uptake, this may also be another reason for the significant decrease in stem dry matter.

Cortical cells of stems had the function of storing nutrients and water, the stems with more cortical cells could have larger water storage space and water content[37,41]. Cambium played a key role in the radial growth of plants and affects the secondary growth stage of plants[42]. In this study, the thickness of

cambium and cortex significantly decreased under all salt treatments, which indicated that salt stress could reduce water storage and radial growth of *B. racemosa*. Xylem and phloem are the main tissue for water transportation and Photosynthate and assimilation transportation and storage, which was important for tolerance to abiotic stress[43,44]. In this study, Xy and Ph under all salt treatments were significantly thicker than that under control, except for Xy under 20‰ and Ph under 40‰ salt treatment, *B. racemosa* could increase xylem and phloem to transport more water, nutrients and assimilating products under salt stress.

Conclusions

The stem dry weight of *B. racemosa* significanlty reduced under high salt stress (30‰ - 40‰), while root, shoot and leaf dry weight did not vary under low salt stress (≤ 25‰), *which* could be related to stable Pn and Ci, increment of Fv/Fm and ΦPSI, the increment or stable palisade tissue and spongy mesophyll of leaf and the increment of epidermis, outer cortex, and stele diameter of root under low salt stress.

Abbreviations

Pn Net photosynthetic rate

Ci Intercellular CO_2 concentration

Gs Stomatal conductance

Tr Transpiration rate

Fv/Fm Quantum yield

NPQ Non-photochemical quenching

ΦPSII PSII actual photo-chemical quantum yield

ΦPSI PSI actual photochemical quantum yield

RDW Root dry weight

SDW Stem dry weight

LDW Leaf dry weight

TDW Total dry weight

R/S Root shoot ratio

Ep Epidermis

Ex Outer cortex

St Stele

Xy Xylem

Ca Cambium

Ph Phloem

Co Cortex

Ue Upper epidermis

Le Lower epidermis

Pt Palisade tissue

Sm Spongy mesophyll

Mb Midrib bund

Pc Parenchymal

P Palisade cell

Declarations

Data availability

The authors confirm that the data supporting the results of this study are available upon request from the corresponding author Pro. Fang Liang (liangfang360@ylu.edu.cn).

Acknowledgments

This research was supported by the Natural Science Foundation of Guangxi Province, China (No. 2022GXNSFBA035540), the National Natural Science Foundation of China (No. 31660226), Guangxi Universities Young and Middle-aged Scientific Research Basic Ability Improvement Project (No. 2022KY0583), the High-level Talent Research Start-Up Fund of Yulin Normal University (No. G2019ZK43), and the Special project for basic scientific research of Guangxi Academy of Agricultural Sciences (No. Guinongke 2021YT143). We thank professor Taiping He for formal identification of *B. racemosa*.

Author Contributions

X.T., C.L. and H.Z. performed the experiments and collected the data. J.H., L.L, and X.Y. analyzed, interpreted the data. J.H. and X.D. wrote the manuscript. J.H. and L.F. acquired the funding. C.B. revised

the manuscript. All authors contributed to the article and approved the submitted version.

Competing interests

The authors declare no competing interests.

Ethics declarations

We had obtained permission to collect plants. All experiments were performed in accordance with relevant guidelines/regulations.

References

1. Tester, M. & Davenport, R. Na+ tolerance and Na+ transport in higher plants. Ann Bot. **91**, 503-527 (2003).
2. Munns, R. Comparative physiology of salt and water stress. Plant Cell Environ. **25**, 239-250 (2002).
3. Munns, R. & Tester, M. Mechanisms of salinity tolerance. Annual review of plant biology. **59**, 651-681 (2008).
4. Liu, B., Wang, X., Li, K. & Cai Z. Spatially resolved metabolomics and lipidomics reveal salinity and drought-tolerant mechanisms of cotton seeds. J Agric Food Chem. **69**, 8028-8037 (2021).
5. Liu, C. *et al*. Salt tolerance in rice: Physiological responses and molecular mechanisms. The Crop Journal. **10**, 13-25 (2022).
6. Van Zelm, E., Zhang, Y. & Testerink, C. Salt tolerance mechanisms of plants. Annu Rev Plant Biol. **71**, 403-433 (2020).
7. Munns, R. & Tester, M. Mechanisms of salinity tolerance. Annu Rev Plant Biol. **59**, 651-681 (2008).
8. Zahra, N. *et al*. Regulation of photosynthesis under salt stress and associated tolerance mechanisms. Plant Physiol Biochem. **178**, 55-69 (2022).
9. Huang, Z., Zhuang, W., Liu, H. & Hu, J. Subduction of a low-salinity water mass around the Xisha Islands in the South China Sea. Sci Rep. **8**, 3074 (2018).
10. Long, X. *et al*. Developing and sustainably utilize the coastal mudflat areas in China. Sci Total Environ. **1**, 1077-1086 (2016).
11. Meena, M. *et al*. Municipal solid waste (MSW): Strategies to improve salt affected soil sustainability: A review. Waste Manag. **84**, 38-53 (2019).
12. Zhao, Y., Wang, L., Zhao, H. & Chen, X. Research status and prospects of saline-alkali land amelioration in the coastal region of China. Chinese Agricultural Science Bulletin. **38**, 67-74 (2022).
13. Fan, H. & Wang, W. Some thematic issues for Mangrove conservation in China. Journal of Xiamen university (Natural science). **56**, 323-330 (2017).
14. Zhen, J., Liao, J. & Shen, G. Mapping mangrove forests of Dongzhaigang Nature Reserve in China using landsat 8 and radarsat-2 polarimetric SAR data. Sensors. **18**, 4012 (2018).

15. Lin, X. *Barringtonia racemosa*–an excellent ornamental tree. Subtropical Plant Science. **27**, 45-47 (1998).
16. Nong, S. & Li, M. Fine ornamental tree species - *Barringtonia racemosa*. Forestry of China. **1**, 39 (2006).
17. Liang, F. *et al*. Effects of flooding on the growth and physiological characteristics of *Barringtonia acutangula*. Journal of Northwest Forestry University. **34**, 48-55 (2019).
18. Liang, F. *et al*. Growth and physiological responses of semi-mangrove plant *Barringtonia racemosa* to waterlogging and salinity stress. Guihaia. **41**, 872-882 (2021).
19. Tan, X. *et al*. Effects of salt stress on growth of *Barringtonia racemosa* and absorption and translocation of mineral elements in it. Journal of Southern Agriculture. **52**, 1887-1898 (2021).
20. Liang, F. *et al*. Physiological response of endangered semi-mangrove *Barringtonia racemosa* to salt stress and its correlation analysis. Journal of Central South University of Forestry & Technology. **39**, 12-18 (2019).
21. Rao, L., Li, S. & Cui, X. Leaf morphology and chlorophyll fluorescence characteristics of mulberry seedlings under waterlogging stress. Sci Rep. **11**, 13379 (2021).
22. Shen, X. *et al*. Interactive effects of single, binary and trinary trace metals (lead, zinc and copper) on the physiological responses of Kandelia obovata seedlings. Environ Geochem Health. **41**, 135-148 (2019).
23. Chen, W. *et al*. Salt tolerance of 5 typical landscape plant species in Zhoushan Islands. Journal of Zhejiang A & F University. **34**, 283-293 (2017).
24. Zou, X., Lie, Z. & Xue, L. Effects of salt stress on biomass of seven landscape plants. Journal of Central South University of Forestry & Technology. **38**, 97-101, 128 (2018).
25. Lie, Z. & Xue, L. Effects of salt stress on tree growth: A review. World Forestry Research. **30**, 30-34 (2017).
26. Zhang, H., Wang, G., Zheng, K. & Zhang, W. Mass–density relationship changes along salinity gradient in *Suaeda salsa* L. Acta Physiol Plant **32**, 1031-1037 (2010).
27. Mu, Y., Lin, J., Mu, C. & Gao, Z. Effects of NaCl stress on the growth and physiological changes in oat (*Avena sativa*) seedlings. Notulae Botanicae Horti Agrobotanici Cluj-Napoca. **43**, 468-472 (2015).
28. Qi, L., Bo, X., Niu, W. & Zhang, Z. Effect of rhizosphere ventilation on growth of cotton seedlings under salt stress. Chinese Bulletin of Botany. **51**, 16-23 (2016).
29. Liu, Z. *et al*. Effects of NaCl stress on growth and photosynthetic characteristics of *Elaeagnus angustifolia* Seedlings. Scientia Silvae Sinicae. **50**, 32-40 (2014).
30. Zhao, X. *et al*. Effects of salt stress on growth and photosynthetic characteristics of *Magnolia wufengensis* grafted seedlings. Scientia Silvae Sinicae. **57**, 43-53 (2021).
31. Zhou, X. *et al*. Effects of salt stress on photosynthetic characteristics of *Gymnocarpos przewalskii* seedlings. Acta Prataculturae Sinica. **32**, 75-83 (2023).

32. Baker, N. Chlorophyll fluorescence: A probe of photosynthesis *in vivo*. Annu Rev Plant Biol. **59**, 89-113 (2008).
33. Zhang, F., Zhang, L. & Gao, D. Osmotic regulation and chlorophyll flurescence characteristics in leaves of clematis species under Saline-alkali stress. Journal of Northeast Forestry University. **50**, 52-56, 62 (2022).
34. Terletskaya, N. *et al*. Drought stress tolerance and photosynthetic activity of alloplasmic lines *T. dicoccum* x *T. aestivum*. Int J Mol Sci. **21**: 1-16 (2020).
35. Zhi, J. *et al*. Effects of compound growth regulators on the anatomy of jujube leaf and fruit. Saudi J Biol Sci. **27**, 3660-3668 (2020).
36. Wang, Y., Xu, Y. & Lu, J. Anatomical response and adaptability of *Glycyrrhiza inflata* to salt stress. Journal of Shihezi University (Natural Science). **39**, 335-340 (2021).
37. Hameed, M., Ashraf, M. & Naz, N. Anatomical adaptations to salinity in cogon grass [Imperata cylindrica (L.) Raeuschel] from the Salt Range, Pakistan. Plant and Soil. **322**, 229-238 (2009).
38. Imada, S., Matsuo, N., Acharya, K. & Yamanaka, N. Effects of salinity on fine root distribution and whole plant biomass of *Tamarix ramosissima* cuttings. Journal of Arid Environments. **114**, 84-90 (2015).
39. Zhang, R., Ma, X. & Lv, H. Response of growth and anatomical structure of roots of *Tamarix ramosissima* seedlings to salinity and water stress. Pratacultural Science. **33**, 1164-1173 (2016).
40. Terletskaya, N. *et al*. Architectural traits in response to salinity of wheat primary roots. Acta Physiologiae Plantarum. **41**, 157 (2019).
41. Reinoso, H., Sosa, L., Ramírez, L. & Luna, V. Salt-induced changes in the vegetative anatomy of *Prosopis strombulifera* (Leguminosae). Canadian Journal of Botany. 82, 689-697 (2004).
42. Matte R., Sun, Y. & Jones, B. The vascular cambium: molecular control of cellular structure. Protoplasma. **247**, 145-161 (2010).
43. Boughalleb, F., Denden, M. & Tiba, B. Anatomical changes induced by increasing NaCl salinity in three fodder shrubs, *Nitraria retusa*, *Atriplex halimus* and *Medicago arborea*. Acta Physiologiae Plantarum. **31**, 947-960 (2009).
44. Hameed, M., Ashraf, M., Naz, N. & Alqurainy, F. Anatomical adaptations of *Cynodon dactylon* (L.) Pers., from the salt range Pakistan, to salinity stress. I. Root and stem anatomy. Pakistan Journal of Botany. **42**, 279-289 (2010).

Tables

Table 1

Root, stem, leaf and total dry weight (RDW, SDW and TDW), and root shoot ratio (RSR) of B. racemosa under salt stress.

Treatments	RDW g	SDW g	LDW g	TDW g	RSR
0 (Control)	1.26 ± 0.05 ab	1.21 ± 0.02 ab	1.12 ± 0.08 a	3.59 ± 0.11 bc	0.54 ± 0.01 a
15‰	1.36 ± 0.02 a	1.32 ± 0.06 a	1.19 ± 0.14 a	3.86 ± 0.19 a	0.55 ± 0.04 a
20‰	1.33 ± 0.10 ab	1.30 ± 0.08 a	1.16 ± 0.02 a	3.79 ± 0.19 ab	0.54 ± 0.02 a
25‰	1.34 ± 0.01 ab	1.13 ± 0.11 bc	1.18 ± 0.05 a	3.65 ± 0.13 abc	0.58 ± 0.04 a
30‰	1.25 ± 0.04 b	1.09 ± 0.02 c	1.10 ± 0.00 a	3.40 ± 0.06 c	0.57 ± 0.01 a
35‰	1.28 ± 0.08 ab	1.09 ± 0.04 c	1.14 ± 0.03 a	3.50 ± 0.09 c	0.58 ± 0.04 a
40‰	1.27 ± 0.05 ab	1.06 ± 0.04 c	1.14 ± 0.05 a	3.47 ± 0.07 c	0.58 ± 0.02 a

Table 2

Net photosynthetic rate (Pn), transpiration rate (Tr), stomatal conductance (Gs); intercellular CO_2 concentration (Ci) of B. racemosa under salt stress. All data in the table show the means with standard deviations (Means ± SD; n = 3). Different lowercase letters indicate that the mean values are significantly different among the treatments at $P < 0.05$ according to Duncan's test. The same as bellow.

Treatment	Pn ($\mu mol\ CO_2\ m^{-2}\ s^{-1}$)	Tr ($mmol\ m^{-2}\ s^{-1}$)	Gs ($mmol\ m^{-2}\ s^{-1}$)	Ci ($\mu mol\ CO_2\ mol^{-1}$)
0 (Control)	4.67 ± 1.16 a	0.50 ± 0.37 a	7.33 ± 4.16 a	601.83 ± 45.73 a
15‰	3.87 ± 1.33 a	0.45 ± 0.16 a	5.33 ± 1.16 a	567.84 ± 0.91 a
20‰	3.71 ± 1.40 ab	0.37 ± 0.07 a	4.67 ± 4 .62 a	564.81 ± 12.77 a
25‰	3.45 ± 1.59 ab	0.34 ± 0.17 a	4.67 ± 2.31 a	556.35 ± 67.90 ab
30‰	3.25 ± 0.51 ab	0.29 ± 0.15 a	4.00 ± 2.00 a	544.21 ± 3.53 abc
35‰	1.71 ± 0.72 b	0.24 ± 0.17 a	3.33 ± 1.16 a	496.97 ± 23.62 bc
40‰	1.63 ± 0.46 b	0.17 ± 0.06 a	2.67 ± 1.16 a	492.20 ± 15.98 c

Table 3
Quantum yield (Fv/Fm), non-photochemical quenching (NPQ), PSII actual photochemical quantum yield (ΦPSII), PSI actual photochemical quantum yield (ΦPSI) of B. racemosa under salt stress.

Treatment	Fv/Fm	NPQ	ΦPSII	ΦPSI
0 (Control)	0.78 ± 0.02 a	3.09 ± 0.75 a	0.11 ± 0.02 a	2.63 ± 0.42 a
15‰	0.75 ± 0.04 ab	2.66 ± 0.19 ab	0.12 ± 0.04 a	2.02 ± 1.00 ab
20‰	0.75 ± 0.04 ab	1.58 ± 0.47 c	0.13 ± 0.04 a	1.62 ± 0.90 ab
25‰	0.75 ± 0.06 ab	2.36 ± 0.46 abc	0.13 ± 0.06 a	2.00 ± 1.43 ab
30‰	0.75 ± 0.01 ab	1.83 ± 0.23 c	0.12 ± 0.01 a	1.69 ± 0.28 ab
35‰	0.68 ± 0.03 ab	2.18 ± 0.26 bc	0.11 ± 0.04 a	0.74 ± 0.12 b
40‰	0.67 ± 0.10 b	1.72 ± 0.37 c	0.10 ± 0.01 a	0.76 ± 0.56 b

Table 4
The thickness of epidermis (Ep), outer cortex (Ex), and stele (St) diameter of B. racemosa root under salt stress.

Treatment (‰)	Thickness of Ep (μm)	Thickness of Ex (μm)	St diameter (μm)
0 (Control)	17.26 ± 0.67 cd	330.88 ± 4.59 a	298.39 ± 10.44 c
15	15.18 ± 10.58 d	283.21 ± 22.43 bc	349.99 ± 30.83 b
20	17.14 ± 1.06 cd	259.21 ± 49.81 c	183.28 ± 10.57 e
25	25.71 ± 3.47 a	123.24 ± 11.42 e	524.65 ± 21.52 a
30	19.16 ± 1.68 bc	307.26 ± 27.24 ab	248.43 ± 22.21 d
35	16.78 ± 1.70 cd	255.66 ± 16.07 c	212.75 ± 23.13 de
40	20.69 ± 2.37 b	201.42 ± 51.13 d	201.76 ± 82.84 de

Table 5

The thickness of xylem (Xy), cambium (Ca), phloem (Ph) and cortex (Co) of B. racemosa stem under salt stress.

Treatment (‰)	Xy (μm)	Ca (μm)	Ph (μm)	Co (μm)
0	2652.96 ± 122.79 c	104.16 ± 18.20 a	487.79 ± 115.84 c	622.48 ± 63.85 a
15	3079.50 ± 45.99 b	70.72 ± 7.26 b	768.11 ± 5 9.92 a	308.64 ± 48.17 c
20	2195.90 ± 137.72 d	48.22 ± 6.93 c	624.42 ± 29.60 b	272.92 ± 63.83 c
25	3236.32 ± 58.85 a	57.61 ± 4.89 bc	782.95 ± 40.31 a	270.71 ± 30.04 c
30	3368.06 ± 208.50 a	55.06 ± 4.81 bc	758.39 ± 51.21 a	268.81 ± 25.42 c
35	3048.83 ± 65.83 b	58.53 ± 25.82 bc	745.44 ± 157.66 a	447.65 ± 107.56 b
40	3274.81 ± 81.32 a	65.15 ± 6.75 b	575.95 ± 2 2.14 bc	488.99 ± 32.06 b

Table 6

The thickness of upper epidermis (Ue), lower epidermis (Le), palisade tissue (Pt), spongy mesophyll (Sm), midrib bund (Mb), and parenchymal (Pc) of B. racemosa leaf under salt stress.

Treatment (‰)	Ue (μm)	Le (μm)	Pt (μm)	Sm (nm)	Mb (μm)	Pc(μm)
0(Control)	23.86 ± 0.81 ab	19.30 ± 1.42 a	67.49 ± 2.16 b	94.37 ± 4.31 bc	105.51 ± 34.35 b	154.31 ± 29.08 a
15	21.94 ± 1.18 cd	18.31 ± 1.64 a	74.18 ± 1.97 a	102.04 ± 4.63 a	158.58 ± 20.02 a	168.88 ± 25.34 a
20	20.74 ± 1.32 d	15.4 4 ± 0.87 b	66.57 ± 2.88 bc	90.67 ± 3.24 cd	144.18 ± 31.59 a	162.23 ± 16.55 a
25	20.67 ± 0.63 d	15.04 ± 1.49 b	62.46 ± 4.88 c	97.75 ± 5.24 ab	97.10 ± 26.57 b	162.19 ± 20.72 a
30	25.12 ± 2.10 a	19.13 ± 1.42 a	69.62 ± 3.73 b	102.17 ± 2.73 a	177.75 ± 49.61 a	180.57 ± 15.23 a
35	21.06 ± 1.30 d	18.69 ± 1.40 a	74.48 ± 3.57 a	85.67 ± 4.93 d	160.14 ± 14.06 a	178.68 ± 42.04 a
40	23.21 ± 1.43 bc	18.38 ± 0.89 a	53.02 ± 2.44 d	96.61 ± 2.88 ab	72.04 ± 10.33 b	146.59 ± 32.74 a

Figures

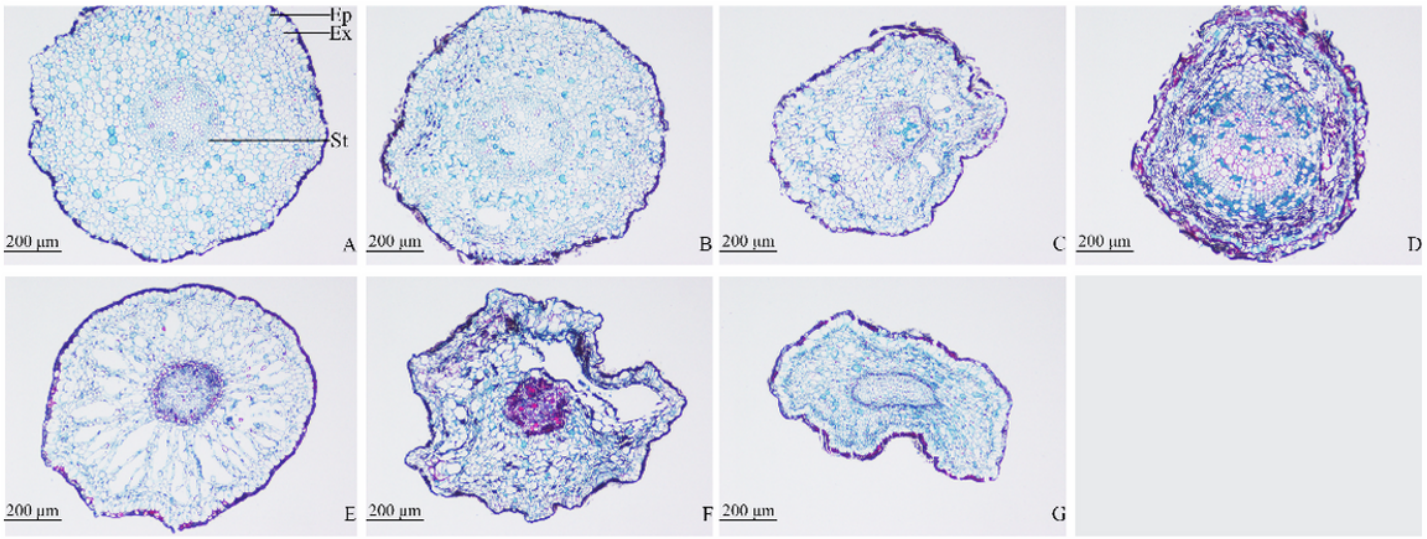

Figure 1

Cross-sections of *B. racemosa* root tip under the control (**A**), 15‰ (**B**), 20‰ (**C**), 25‰ (**D**), 30‰ (**E**), 35‰ (**F**) and 40‰ (**G**) salt treatments. Ep, epidermis; Ex, outer cortex; St, stele. Scale bars = 200 μm.

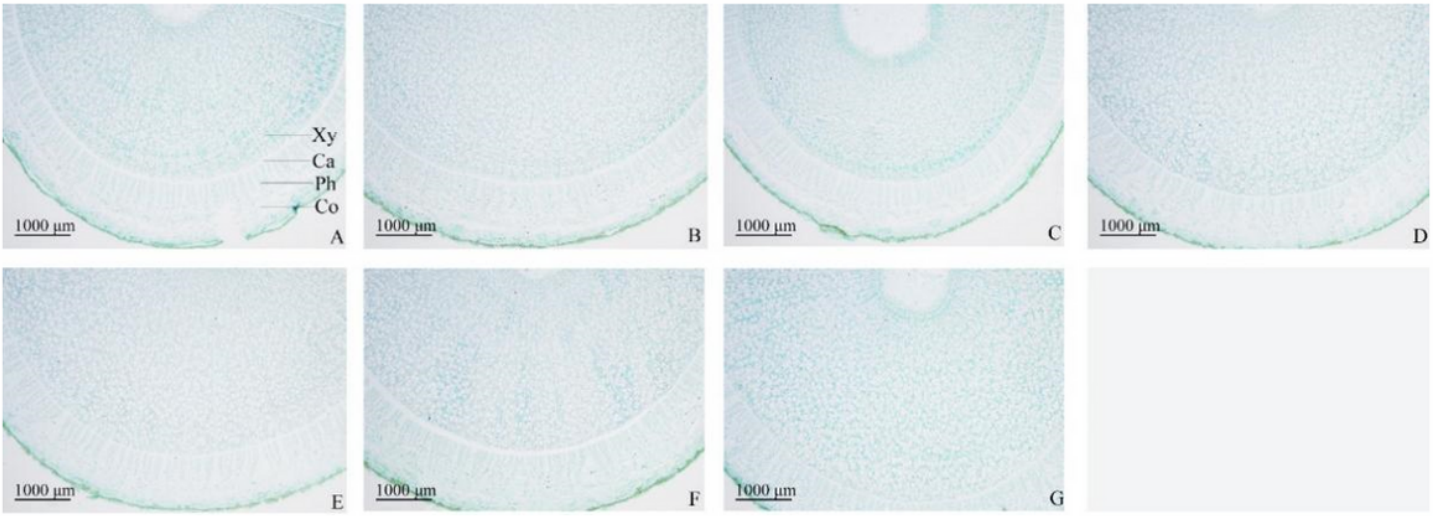

Figure 2

Cross-sections of *B. racemosa* stem under the control (**A**), 15‰ (**B**), 20‰ (**C**), 25‰ (**D**), 30‰ (**E**), 35‰ (F) and 40‰ (**G**) salt treatments. Xy, xylem; Ca, cambium; Ph, phloem; Co, cortex. Scale bars = 1000 μm.

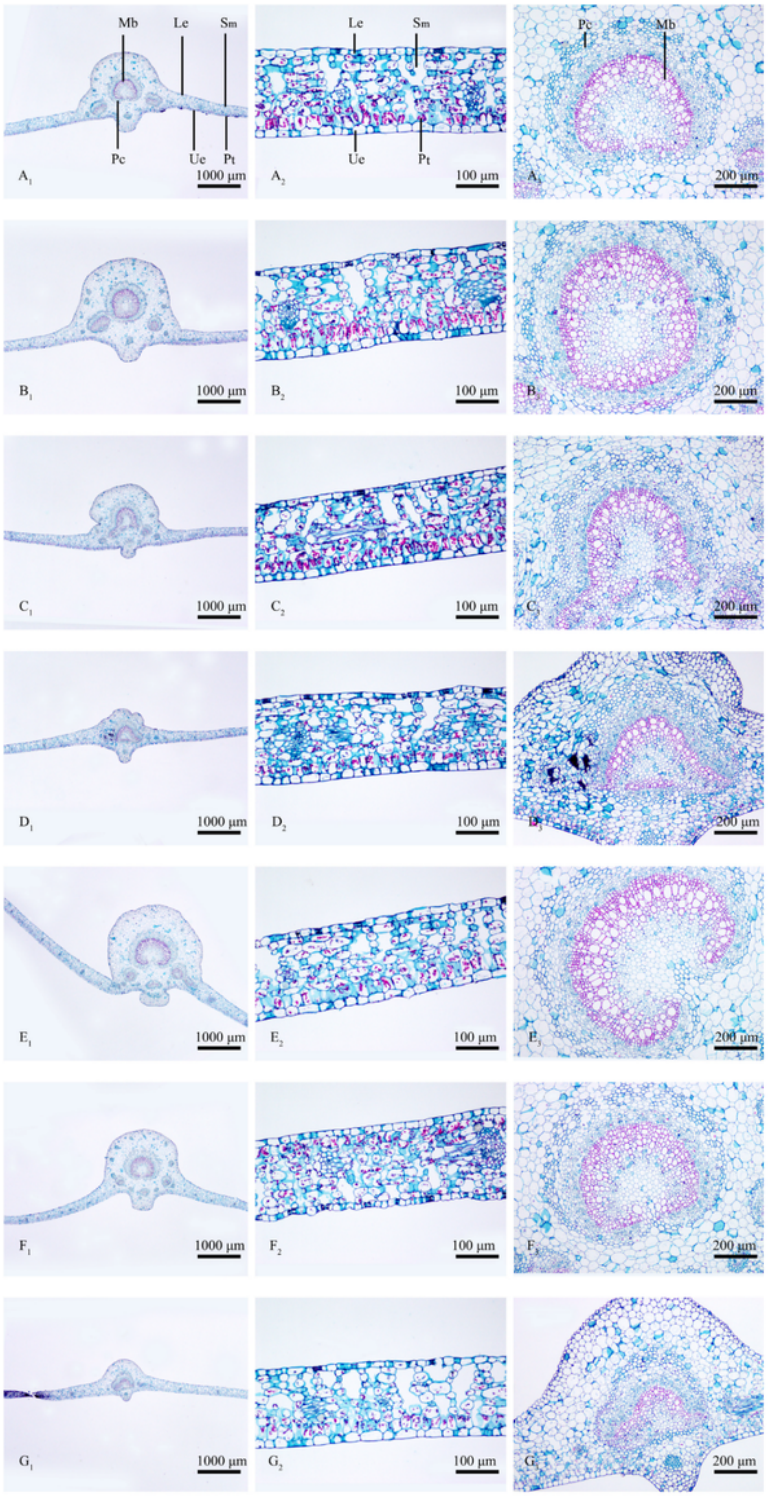

Figure 3

Cross-sections of whole leaf (**A_1** - **G_1**), leaf-bade (**A_2** - **G_2**) and midrib (**A_3** - **G_3**) of *B. racemosa* leaf under the control (**A_1**, **A_2**, **A_3**), 15‰ (**B_1**, **B_2**, **B_3**), 20‰ (**C_1**, **C_2**, **C_3**), 25‰ (**D_1**, **D_2**, **D_3**), 30‰ (**E_1**, **E_2**, **E_3**), 35‰ (**F_1**, **F_2**, **F_3**) and 40‰ (**G_1**, **G_2**, **G_3**) salt treatments. P, palisade cell; Ue, upper epidermis; Sm, spongy mesophyll; Le, lower epidermis; Mb, midrib bund; Pc, parenchymal. Scale bars = 1000, 100, 200 μm, respectively.

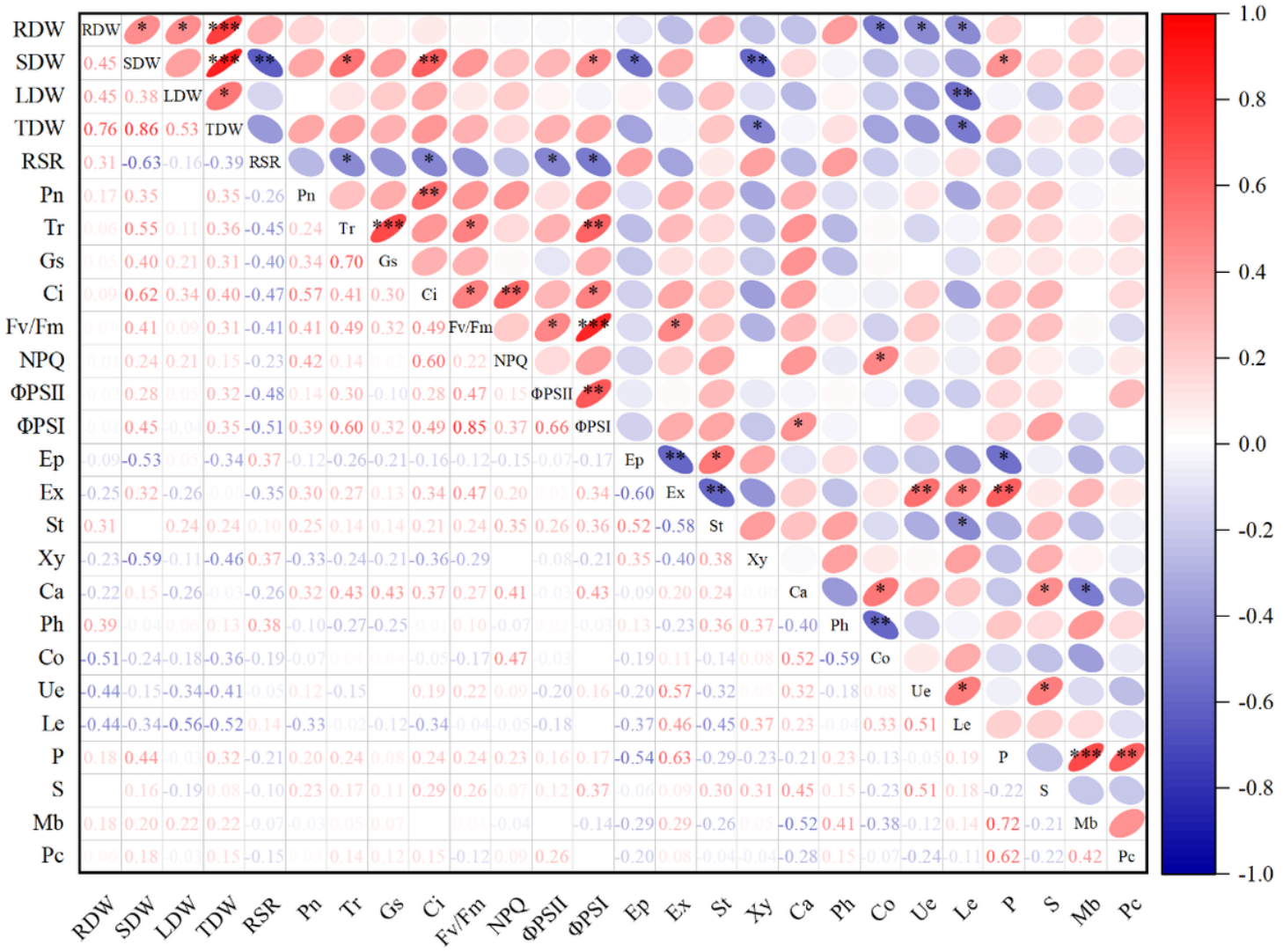

Figure 4

Pearson correlation matrix between photosynthetic and fluorescence parameters and dry weight, root to shoot ratio. Significant values marked with * ($P \leq 0.05$), ** ($P \leq 0.01$) and *** ($P \leq 0.001$). Colors indicate the level of correlation (r) from positive correlation (red) to negative (blue). Variations in the color of blue and red indicate the level of significance. RDW, Root dry weight; SDW, stem dry weight; LDW, leaf dry weight; TDW, total dry weight; RSR, root shoot ratio; Pn, Net photosynthetic rate; Tr, transpiration rate, Gs, stomatal conductance; Ci, intercellular CO_2 concentration; Fv/Fm, Quantum yield; NPQ, non-photochemical quenching; ΦPSII, PSII actual photochemical quantum yield; ΦPSI, PSI actual photochemical quantum yield; E, epidermis; Ex, outer cortex; St, stele; Xy, xylem; Ca, cambium; Ph, phloem; Co, cortex; P, palisade cell; Ue, upper epidermis; Sm, spongy mesophyll; Le, lower epidermis; Mb, midrib bund; Pc, parenchymal.